IEEE Access
Multidisciplinary ⋮ Rapid Review ⋮ Open Access Journal

Received June 5, 2020, accepted June 18, 2020, date of publication June 24, 2020, date of current version July 3, 2020.

Digital Object Identifier 10.1109/ACCESS.2020.3004611

Fuzzy Logic Power Management Strategy for a Residential DC-Microgrid

JULIO C. PEÑA-AGUIRRE[1], ALEJANDRO-ISRAEL BARRANCO-GUTIÉRREZ[2], (Member, IEEE), JOSÉ A. PADILLA-MEDINA[1], ALEJANDRO ESPINOSA-CALDERON[3], (Member, IEEE), AND FRANCISCO J. PÉREZ-PINAL[1], (Senior Member, IEEE)

[1]Tecnológico Nacional de México, Instituto Tecnológico de Celaya, Celaya 38010, México
[2]CONACYT, Instituto Tecnológico de Celaya, Celaya 38010, México
[3]CRODE Celaya, Tecnológico Nacional de México, Celaya 38023, México

Corresponding author: Francisco J. Pérez-Pinal (francisco.perez@itcelaya.edu.mx)

This work was supported in part by the Tecnológico Nacional de México, Instituto Tecnológico de Celaya, and in part by the Consejo Nacional de Ciencia y Tecnología (CONACYT) under Grant Chair 1641. The work of Julio C. Peña-Aguirre was supported by the CONACYT through the Ph.D. Grant.

ABSTRACT Power management strategies (PMS) are applied to keep a balance, between different energy sources (i.e. solar, wind, geothermal, hydro), storage units (i.e. fuel cell, batteries, fly wheel) and loads. Up to date, there has been reported several advance techniques to solve this task, for instance: Fuzzy Logic, Deep Learning, Droop Control, Bayesian Networks, among others. Nevertheless, some of those PMS are over simplified and others are too complex to be programmed in devices with limited resources. To solve these issues, this paper proposes a PMS based on Fuzzy Logic, which keeps a balance between those two goals. Characteristics of the proposed PMS are a small number of rules; fulfillment of the demanded power at every time; reducing use of the storage unit; and keeping a balance between the different sources, storage unit and loads. The proposed PMS is numerically evaluated by using SIMULINK-MATLAB®, in a 10kW residential DC Microgrid (MG), and validated by using a Hardware in the Loop platform (NI myRio-1900 and Typhoon HIL402). A comparison with three popular advance techniques demonstrates the feasibility of the proposed PMS.

INDEX TERMS Power management strategy, DC microgrid, power, storage, renewable energy, energy balance.

I. INTRODUCTION

In October 2018, the Intergovernmental Panel on Climate Change (IPCC), published a report about climate change and the impact of carbon dioxide (CO_2) emissions; the meeting concluded the importance of reducing CO_2 emissions by at least 45% before 2030, otherwise the consequences could be irreversible [1].

One alternative to solve this issue is the implementation of Distributed Generation (DG), DG is an approach that uses small-scale technologies to produce energy close to users [2]. Some DG technologies are modular and based on renewable energy; offering several potential advantages. For instance: the production of energy at lower cost, greater reliability, security, and low environmental impact compared to traditional generation systems [3]–[5]. Another technology used to reduce CO_2 emissions is the smart grid (SG). To understand this concept, it is necessary to remember that traditional grid consists of transmission lines, transformers, and substations, among other components that the provider needs for sending electric power from power generation plants to the end user. Although the main grid is considered a marvel of engineering, currently this approach is over exploited, and it is required another type of grid, one that incorporates the existing technology and overcome current and future issues [6], [7].

In order to understand the term smart and its relationship with the main grid, there is an analogy with digital technology, which allows a bidirectional communication between companies and customers, and the detection along the transmission lines is what makes the smart grid. Such as the Internet, the SG consists of controls, computers automation

The associate editor coordinating the review of this manuscript and approving it for publication was Sanjeevikumar Padmanaban.

and new technologies that work together, but in this case, these technologies work with the main grid to respond digitally to an electricity demand that changes very fast and continously. Indeed, the SG represents an opportunity to change the traditional power grid to a network that guarantees flexibility, security, efficiency and reduces the environmental impact [8], [9].

On the other hand, a microgrid (MG) is a discrete system, which consists of DG sources (storage and generation) and loads, capable of operating with or without the power grid. Up to date, there are different types of MG for instance: intensive battery bank (BB). Those based on photovoltaic panels or by wind generators, other incorporates a hydrogen storage system or supercapacitors (SC), and a combination of those can be also found in [43]–[45]. To coordinate a MG, it is used a management strategy (energy, power or both); and the main objective for this technology is to guarantee the supply of electric power, while also providing solutions for residential or industrial use [10]–[13]. A MG has similar characteristics to the traditional power grid. However, the MG provides proximity between energy generation and energy use, resulting in an increasing efficiency and a significant reduction of transmission losses [14]–[21], [45].

The dynamic control of the MG allows dependence of main grid during normal operation or peak demands, and once the main grid fails, the MG can operate with autonomy. In this situation, the control isolates the fault without affecting its integrity and performance [7], [22], [23]. The case like the above is an example of a power management strategy (PMS), which can help to improve the system's performance and protection.

Some principal PMS's objectives are shown below: a) to meet the load demand at overall time, b) to maximize the use of the generated energy, c) to minimize the use of the power grid, d) to store the generated energy, and e) to extend the life of the energy storage systems [24]–[29]. Indeed, addition of goals and prioritizing one over another in practical PMS relies on several factors, for instance: isolation or non-isolation, AC or DC application (i.e. residential, industrial, maritime, etc.), regulations of each country or region, economy factors, and interfacing topology of power electronics, among others [30]–[36].

The PMS is quite flexible and it varies in the type of control, operation, and architecture. For instance, one can find those based on storage capacity, which are controlled by a centralized, decentralized or a hybrid technique. Indeed, PMS can also be classified by the kind of empirical strategy used, which are usually developed from previous system's knowledge by trial error [45], [46], by Boolean rules or by states machines. PMS techniques found in literature include: Droop control, Bayesian networks, Fuzzy control, or Multi-agent architecture, to name a few [37]–[42].

Nowadays, three popular Fuzzy Logic strategies (FL) used as PMS are the Fuzzy Logic Control based on Net Power Trend (FLC NPT) [49], the Fuzzy Logic Control based on Energy Rate of Charge (FLC ERC) [50], and the Fuzzy Logic Control based on Grid Fluctuation (FLC GF) [54]. In the FLC NPT, the diffuse controller considers the tendency of the power flow in the MG to minimize the power exchange with the main grid; while extending the life of the storage unit against the charging and discharging cycles. On the other hand, the FLC EROC strategy reduces the controller's complexity, and minimizes power peaks and fluctuations in the power grid while maintaining the state of charge within safe limits. Finally, FLC GF strategy focuses on the management of the storage system to reduce the fluctuation of the power demanded to the grid.

Besides their reported advantages, unfortunately, some of them simplifies the MG structure and others are too difficult for a real-time implementation. In order to solve such concerns, this paper is proposed a PMS based on Fuzzy Logic, which keeps an equilibrium between MG construction and complexity. Some advantages of this of this system are a slight number of rules, satisfaction of the demanded power at overall time, diminishing use of the storage unit, and equilibrium among sources, storage unit and loads. To evaluate the proposed system, a 10kW residential DC Microgrid (MG) is selected, which is numerically assesed by using Simulink-MATLAB®, and evaluated by using Hardware in the Loop (Typhon HIL402). A quantitative comparison with the three popular FL techniques is also reported.

II. RESIDENTIAL MG

The residential non-isolated MG considered as a benchmark was based on reference [47]. This system is shown in Figure 1 and it consists of five sections.

The first one is the main energy source, which consists of an array of 15 × 100 Solartech® polycrystalline solar panels 12V, 100W connected in series/parallel to develop a 10 kW, 190V DC bus. This bus is linked to a 10 kW, 190V DC to 380V DC step-up converter, which operates with a maximum power point tracking (MPPT) algorithm. The second section is a storage unit, which consists of an array of 15 × 6 standard absorbed glass mat (AGM) deep cycle batteries of 12V, 1.62 kWh with passive equalization. This array was connected in a series/parallel to create a battery bank (BB) bus of 10kW, 190V DC, and linked to a $190VDC/380VDC$ bidirectional converter. The third section is a bidirectional $380VDC/220V$ rms to 60 Hz inverter/rectifier. The fourth section consists of typical office devices (computers, laptops, printers, luminaries, furnace and refrigerator) which together has a load power of 8 kW. The final section was the 220V rms to 60 Hz main grid.

Figure 1 shows that energy flows are considered positive according to the direction of the arrows, where power grid and MG power (P_{MG}) are expressed as follow:

$$P_{Gen} = P_V - P_{MG} \pm P_{Bat} \quad (1)$$

$$P_{MG} = P_{Load} \pm P_{Grid} \quad (2)$$

where P_{Load} is the MG load power, P_{Gen} is the generated power by the solar array (P_V), and P_{Bat} is the BB power.

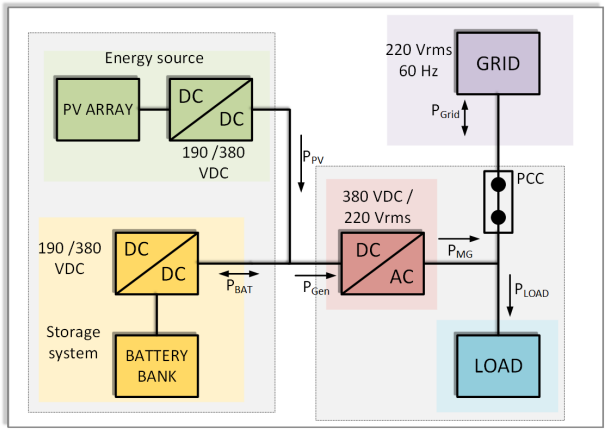

FIGURE 1. DC Microgrid of 10*kW*.

P_{Bat} directly affects the state of charge (SOC) from BB, which should be kept, within the bounds of safety, $SOC_{min} \leq SOC \leq SOC_{max}$, in order to extend the BB's life. The SOC is defined by the following expression [48]:

$$SOC(n) = SOC(n-1) \pm \frac{1}{AHC} \int_{t_0}^{t} i(\tau) d\tau \qquad (3)$$

where $SOC(n-1)$ is a state of previous charge, AHC is the capacitance of the battery fully charged, $i(\tau)$ is the current load $(+)$ or $(-)$.

For case studies, it is assumed that the power drawn by the photovoltaic arrays is the maximum that can be generated, and the AC loads are not controllable [48]. In contrast with the power exchanged with the main grid that can be controlled by a directional rectifier/inverter; while the batterie's charging is controlled.

P_{Load} (Figure 2a) and the P_{Gen} (Figure 2b) were monitored from July 2017 to October 2017 with the help of the power analyzer, Carlo Gavazzi WM40, with sampling time of 15 min (900 *sec*) for four months.

Figure 3 shows the P_{MG} data acquired with the analyzer, later these data are used for the design of the PMS.

III. PROPOSED FUZZY CONTROLLER

A. CONTROL STRATEGY

The main objective of the proposed fuzzy logic PMS is to maintain a balance between the generated and demanded power, to reduce the use of the BB and the main grid, and to reduce the number of diffuse rules. Authors called to this strategy Fuzzy Logic Equilibrium Power Controller (FL EPC).

Figure 4 shows this proposal and it considers the P_{Grid} as the difference between the output of the EPC and P_{Net}, and P_{Bat} is the addition between P_{Grid} and P_{Net}. The P_{Net} represents the difference between P_{MG} (Figure 3) and P_{Load} (Figure 2a) and it is also an input for FL EPC.

$$P_{Grid} = P_{Net} - P_{FL\ EPC} \qquad (4)$$

$$P_{Bat} = P_{Grid} + P_{Net} \qquad (5)$$

$$P_{Net} = P_{MG} - P_{Load} \qquad (6)$$

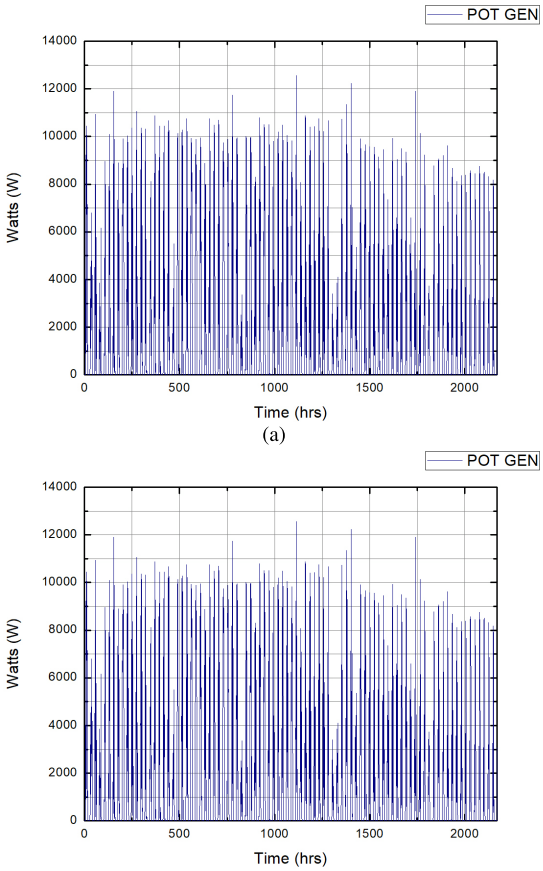

FIGURE 2. Power data. (a) P_{Load} data. (b) P_{Gen} data.

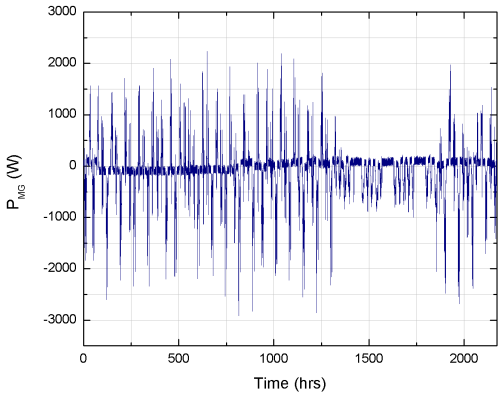

FIGURE 3. DC Microgrid power data.

where $P_{FL\ EPC}$, represents the output from the fuzzy logic controller (FLC), which has two inputs: SOC and P_{Net}. The FLC uses also the SOC as an input for monitoring the BB's SOC_{max} and SOC_{min}.

Furthermore, P_{MG} provides information to FL EPC on the power inputs and outputs of the MG.

With both inputs from FL EPC increases, decreases or maintains the power absorbed/injected into the main grid and simultaneously satisfy P_{Load}.

The control diagram for this strategy is shown in Figure 4. P_{Grid} and P_{Bat} corresponds to equations 4 and 5, respectively. Figure 4 also shows SOC estimator represented by equation 3.

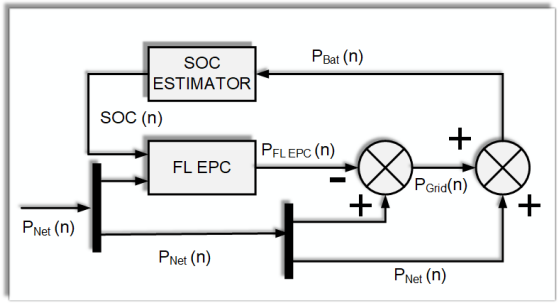

FIGURE 4. FL EPC control diagram.

B. FL EPC DESIGN

The FL EPC block shown in Figure 4, consists of a diffuse Mamdani type with a defuzzyfication based on center of gravity (COG), and with two inputs and one output, P_{MG} and SOC respectively. Also this controller consists on a set of fuzzy rules "$IF-THEN$", where the system takes as input the values of the fuzzyfication and it applies to the background. The AND and OR operator is used to obtain a singles number that represents the evaluation result.

This number (the truth value) applies to the consequence [51], [52]. The advantages of using this type of fuzzy system: a) it is very intuitive, b) it could be trained by an artificial neural network or by hand, and c) it is adapted to incorporate knowledge and experience.

The defuzzyfication by COG transforms the diffuse output into a real number; this technique is widely used and recommended for control development [53].

The procedure followed for the design of this FL EPC was:

1) Set the inputs and outputs, MF (membership functions): type, name and rank.
2) Set the rules of the FL EPC.
3) Adjust for the MF of the inputs and outputs, using actual data presented in section II.
4) Optimize initial rules, using real acquired data, and minimize the rules used in FL EPC.

The membership functions of the FL EPC are; $\mathcal{L}P_{NET} = \{NB, NS, Z, PS, PB\}$ where are "NB" Negative Big, "NS" Negative Small, "Z" Zero, "PS" Positive Small, and "PB" Positive Big as shown in the Figure 5a and $\mathcal{L}SOC = \{CF, CM, CN\}$ where are "CF" Charge Full, "CM" Charge Medium, and "CN" Charge Null as seen in the Figure 5b; the linguistic variables for $\mathcal{L}P_{NET}$ are $NB_j(x) = (-1.4\ X10^4, -3333, -3000)_R$, $NS_j(x) = (-3000, -2000, -100, 0)_{LR}$, $Z_j(x) = (0, 300)$, $PS_j(x) = (266.7, 2000, 3000)_R$, and $PB_j(x) = (3000, 3333, 1.4\ X10^4)$.

While the linguistic variables for $\mathcal{L}SOC$ with $CN_j(y) = (0, 45, 65)_R$, $CM_j(y) = (55.14, 65.14, 80.14, 90.14)_{LR}$, $CF_j(y) = (85.29, 90.29, 100.3)_L$.

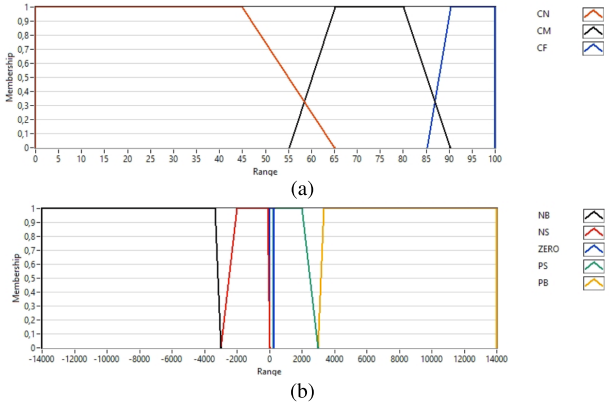

FIGURE 5. Member functions inputs. (a) $SOC'sMF$. (b) $P'_{MG}sMF$.

The output MF from the controller is $\mathcal{L}P_{FLC} = (INY, DESC, RECT)$ as shown in Figure 6, which are "REC" rectify, "INY" inject and "DESC" disconnect.; In this same figure, the MF types used for the output are observed, which are Gaussian (INY, and RECT) and triangular (DESC). The operating range in the output variable is defined according to the maximum power MG can control the FL EPC.

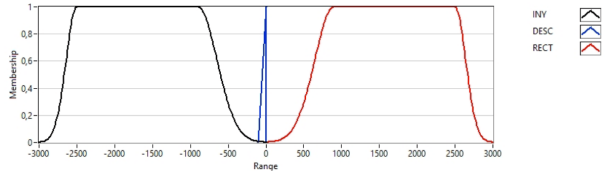

FIGURE 6. Member functions output from P_{FLC}.

The ranges of the linguistic variables from each MF input and output were programmed according to the experience of the programmer in this type of system.

Table 1 shows the distribution of the fifteen fuzzy rules proposed in the FL EPC design. Figure 7 shows the representation from the rules in a 3D graph, x-axis indicates the possible values of SOC, the y-axis illustrate possible values of P_{NET}, and the z-axis shows the results associates with P_{FLC}.

TABLE 1. FLC rule base.

		P_{NET}				
		NB	**NS**	**Z**	**PS**	**PB**
SOC	**CN**	DESC	DESC	DESC	REC	REC
	CM	INY	DESC	DESC	REC	REC
	CF	INY	INY	DESC	REC	REC

IV. NUMERICAL RESULTS

The FL EPC simulation described above, was evaluated with actual data from July 2017 to October 2017. The results were obtained with the use of MATLAB® using the parameters shown in Table 2.

Figure 8 shows the FL EPC performance, during the simulation, where the variation of P_{Bat}, wich has numbers favorable for the SOC and remains within the limits of 50%

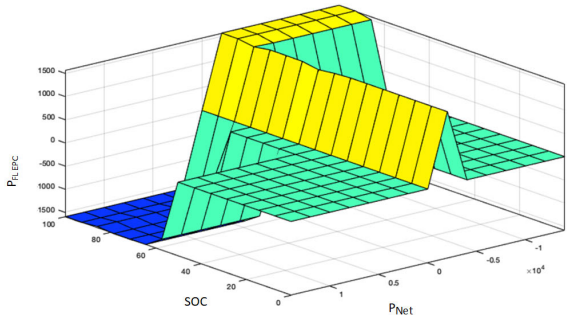

FIGURE 7. 3D visualization of the FL EPC.

TABLE 2. Simulation parameters.

Symbol	Description	Unit
M	Number samples per day	96 samples
N	Total samples	2170 samples
P_{Gen}	Photovoltaic	10 kW
P_{Load}	Consumed	8kW
T_S	Sampling	900 sec
SOC_{max}	Maximun SOC	100 %
SOC_{min}	Minimum SOC	50%

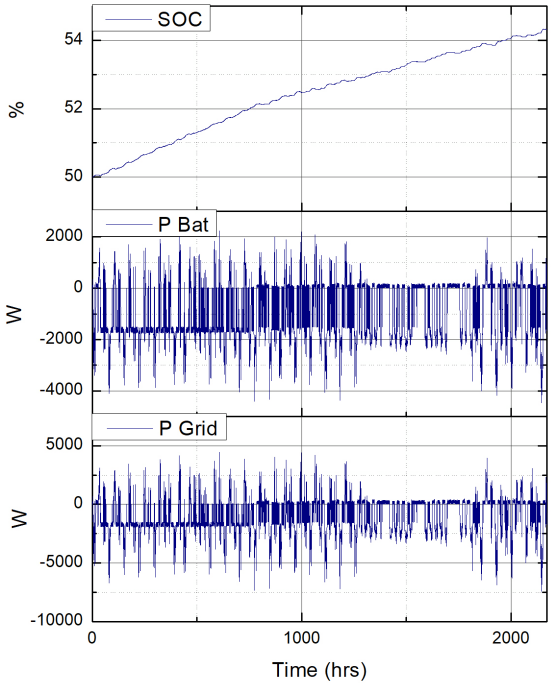

FIGURE 8. FL EPC results.

and 100%. However this did not show a significant change, in addition, the peaks of power are $-4kW$ and $2kW$; on the other hand, P_{Grid} has peaks of power between $-5kW$ and $5kW$ indicating a balance between the power injected and the power rectified [49], [50], [54].

V. HIL VALIDATION

For the validation of each of the techniques mentioned below, the Typhoon HIL402 target was used, which allows us emulating the proposed system. Figure 9 shows the physical connection between Typhoon HIL402 and NI myRio 1900.

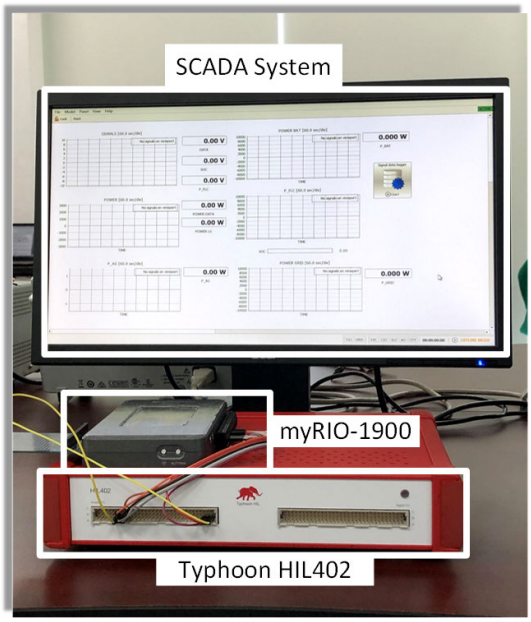

FIGURE 9. Connection scheme.

A NI myRio 1900 was used for, the execution of the PMS in an embedded way since the Typhoon HIL402 card does not have the possibility of executing the FLC, in a cycled time. Since the main feature of myRio 1900 is the simulation of the systems in real time, for this particular case study, the simulation of a residential microgrid. As shown in Figure 9, communication between the two cards is just the input/output connection of both cards, along with signal conditioning.

The data that was used for the simulation in Typhoon HIL402, is shown in Table 3. The simulation time for this validation is 150 hrs, which is approximately one week.

TABLE 3. Simulation parameters Typhoon HIL402.

Symbol	Description	Unit
M	Number samples per day	96 Samples
N	Total of samples	600 Samples
T_s	Sampling Simulated	1 sec

The input power data with which the strategies were tested are those shown in the Figure 10.

The proposed system was also compared with three popular fuzzy logic techniques. Figure 11 shows the block diagrams of the programming for each energy strategy. Each of the strategy diagrams were programmed into the myRio 1900.

The first strategy is FLC NPT (Fuzzy logic controller based on Net Power Trend) [49], [51]. The diffuse controller of this strategy considers the tendency of the power flow in the MG to minimize the power exchange with the main grid; while extending the life of the BB against the charging and discharging cycles, Figure 11 (a).

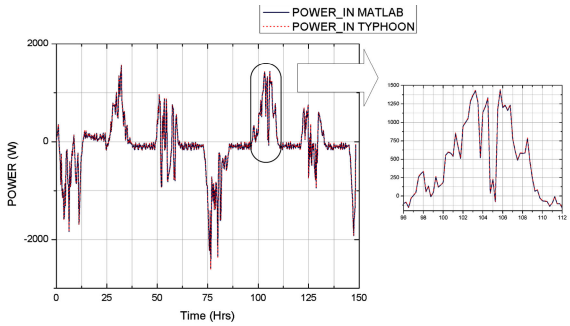

FIGURE 10. Input power.

The second strategy is FLC EROC (Fuzzy logic controller based on Energy Rate of Charge) [50], [51]. It aims at minimizing power spikes and fluctuations in the power grid while maintaining the SOC within safe limits, and reducing the complexity of the FLC, Figure 11 (b).

The last strategy is the EMS proposal [54], instead of using the grid control approach, the paper focuses on the management of the BB's storage system only and uses it to reduce the fluctuation of the P_{Grid} in a MG, Figure 11 (c).

Table 4 shows a comparison between the number of fuzzy rules used in each FLC, the number of inputs and outputs, and other implementation parameters. This same table also shows the difficulty of implementation, being the most complex by the rules and by the number of inputs the FLC NPT, since it is using 3 inputs and 50 rules for its execution. Likewise, the FLC EROC and FLC GF are among the strategies whose difficulty is medium, due to the number of rules they use; while the proposed strategy has the advantage of fewer rules, which translates into less use of the computational resources, and less amount of memory used.

TABLE 4. Comparison PMS's.

	FLC NPT	FLC EROC	FLC GF	FL EPC
Fuzzy rules	50	25	35	15
Inputs	3	2	2	2
Outputs	1	1	1	1
Implementation difficulty	Hard	Medium	Medium	Easy
Memory (KB)	62	47	61	40
Sample time (sec)	1	1	1	1

A. HIL FLC NPT

Figure 12 shows the comparison between MATLAB®-SIMULINK and Typhoon HIL402 in P_{Bat}, where the simulation with the Typhoon HIL402 at 75 hours shows a peak of 20kW while in that time on the SIMULINK simulation is 2.5 kW.

Despite the great difference, the SOC performance is not as severely affected as it is the sample in Figure 13, which in the mentioned time only suffers a decrease of 0.3% which would correspond to lees than 0.1% of the relative error.

Close to 80 hrs, the P_{Grid} undergoes a change in its performance, as shown in Figure 14. However, this behavior is affected since a peak power close to $-1.2kW$ was obtained in

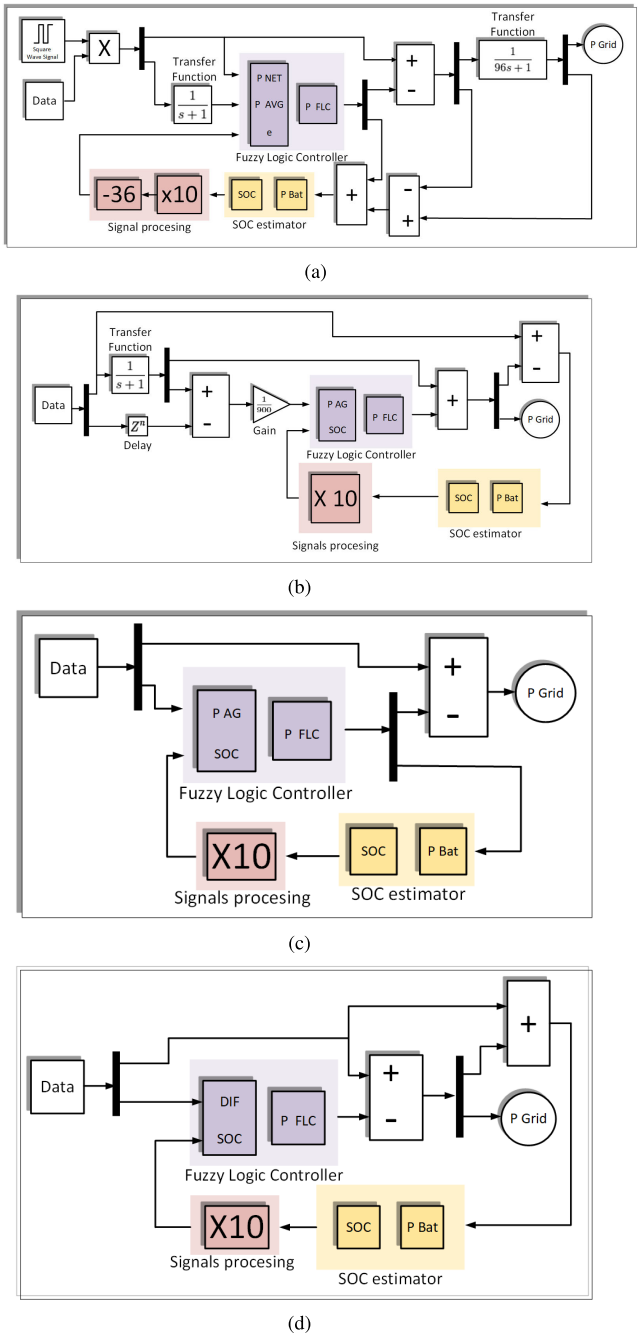

FIGURE 11. Block diagram. (a) FLC NPT. (b) FLC EROC. (c) FLC Grid Fluctuation. (d) FL EPC.

the simulation with the Typhoon HIL402; while the simulation that was carried out in MATLAB® at that same moment registered a power of 4.5 KW.

B. HIL FLC EROC

The second strategy that was simulated in the Typhoon HIL402 was FLC EROC. Figure 15 shows the behavior of the P_{Bat}, where the difference between the two results is the noise observed in the power obtained by the Typhoon HIL402, while the power shown by the MATLAB® platform has a

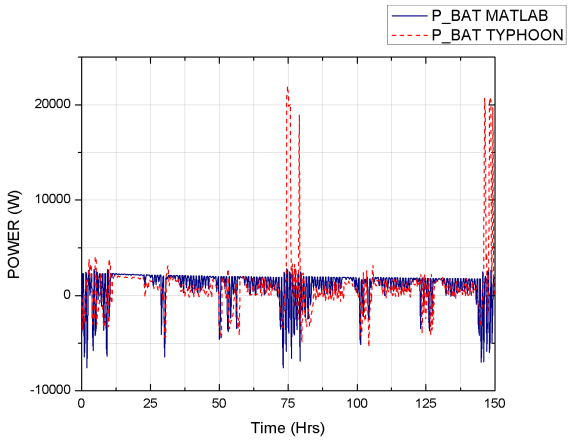

FIGURE 12. P_{Bat} FLC NPT.

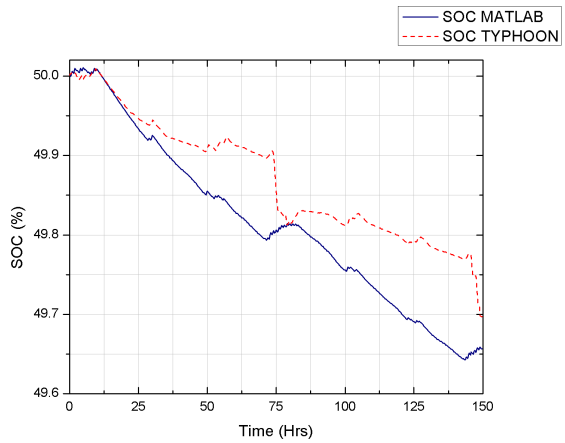

FIGURE 13. *SOC* FLC NPT.

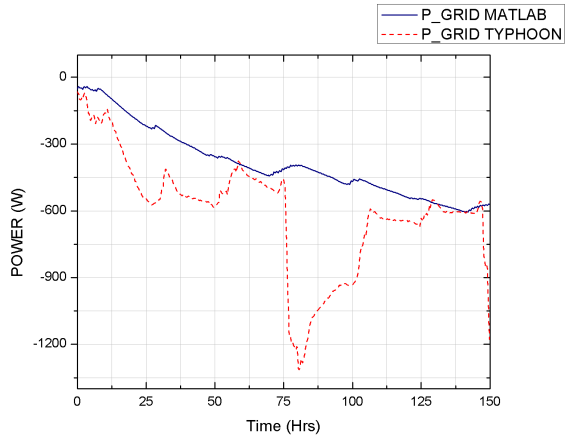

FIGURE 14. P_{Grid} FLC NPT.

cleaner signal of noise. In the meantime it exhibits similar behavior on both simulation platforms.

Despite the noise of the P_{Bat} signal, the *SOC* did not show much difference between the two simulations, as shown in the Figure 16.

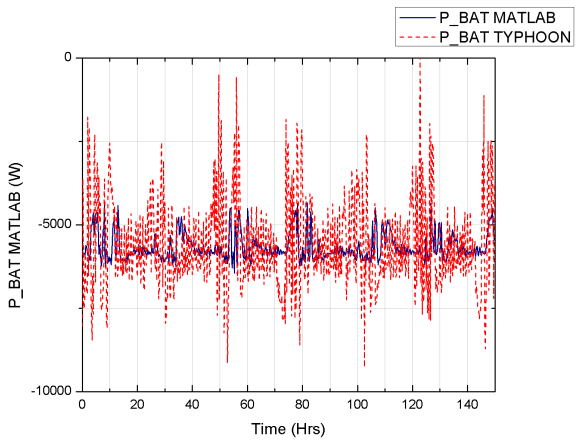

FIGURE 15. P_{Bat} FLC EROC.

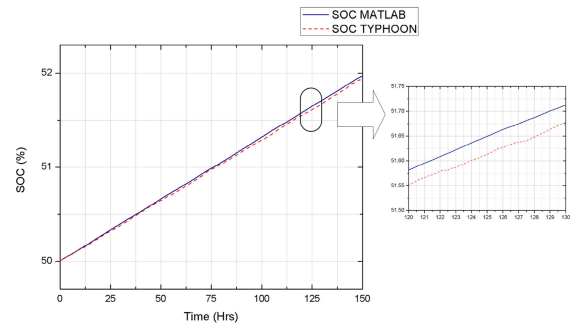

FIGURE 16. *SOC* FLC EROC.

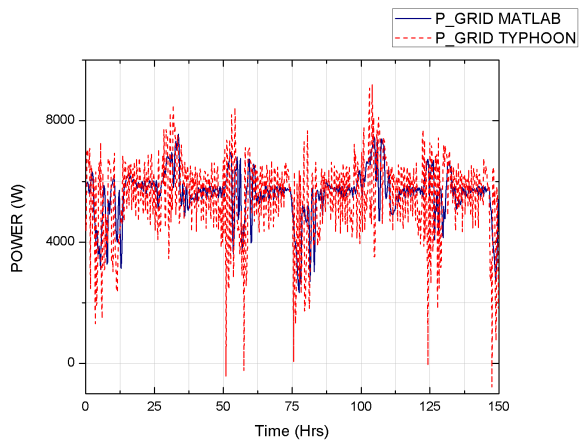

FIGURE 17. P_{Grid} FLC EROC.

Figure 17 shows the FLC EROC P_{Grid} has one of the same characteristics as the Figure 15, as the noise that the signal possesses. However, the behavior of both simulations is preserved.

C. HIL FLC GF

Figure 18 shows the P_{Bat} performance, where the behaviors in both simulations of the strategy are very similar, and the difference between the graphs is small.

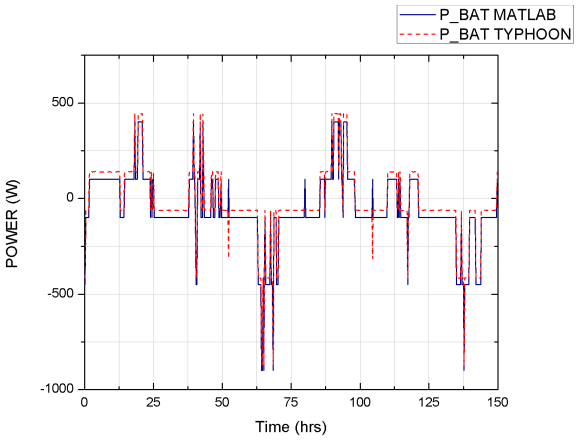

FIGURE 18. P_{Bat} FLC GF.

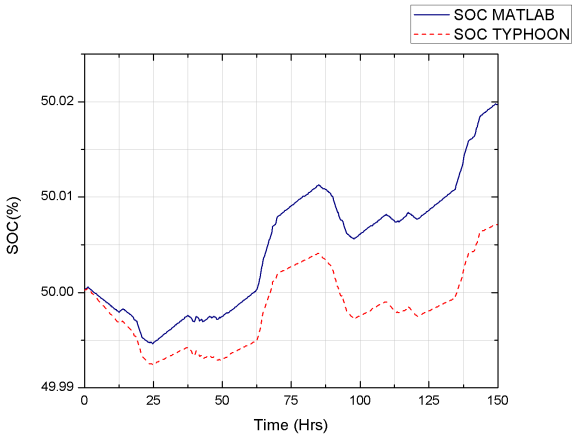

FIGURE 19. *SOC* FLC GF.

With the P_{Bat} the *SOC* was estimated, which is shown in Figure 19, although the Figure shows a wide difference, a relative error of 0.027% is obtained, which is interpreted as a high similarity.

The behavior of P_{Grid}, is shown in Figure 20, comparing the simulated strategy in MATLAB® with the same strategy in Typhoon HIL402, They are are similar except for a power peak between 50 and 75 hours of simulation. On the other hand, MATLAB's strategy shows a peak of 1.8 kW while in that of the Typhoon HIL402 the power peak is 2 kW which translates into a relative error of 10%; which indicates its similarity on both platforms.

D. HIL FL EPC

Another of the strategies of which the platform migration was FL EPC. Figure 21, which shows the behavior of the P_{Bat}.

Even though the magnitudes of the P_{Bat} are not the same because the noise on the signals can do another behavior, it is similar and the *SOC* is the same as shown in Figure 22.

The behavior of the P_{Grid} is shown in Figure 23, which, like the P_{Bat} (Figure 21) is very similar to the one expected in MATLAB.

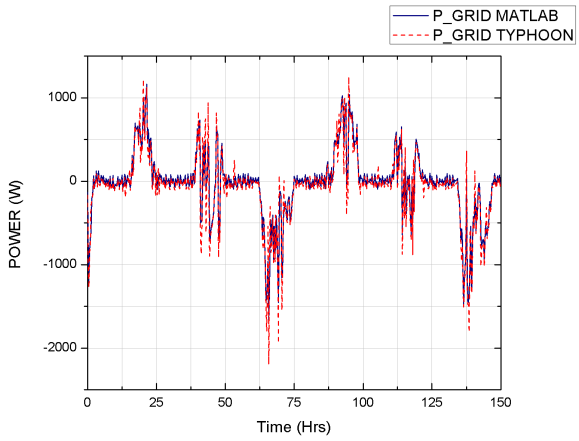

FIGURE 20. P_{Grid} FLC GF.

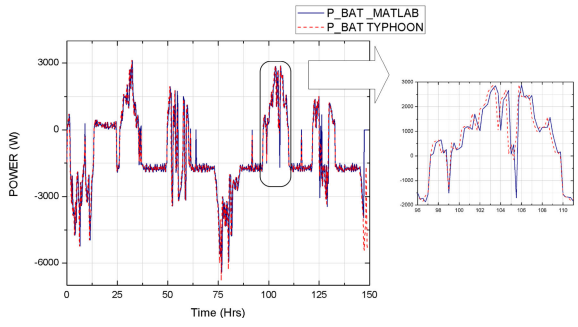

FIGURE 21. P_{Bat} FL EPC.

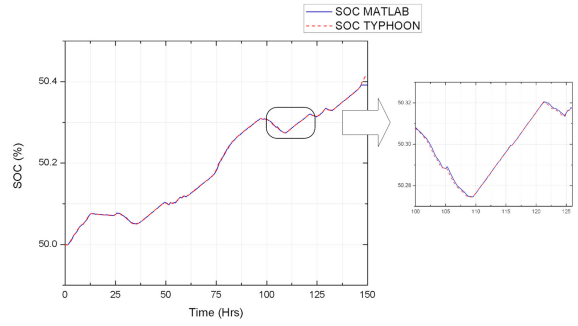

FIGURE 22. *SOC* FL EPC.

VI. DISCUSSION

The main objetive of the administrator is to meet the MG demand either with the power from the photovoltaic arrangement or with the power from the network.The reason to choose the parameters is the control over the signals like P_{Bat} and P_{Grid} and it means a type of stability over each PMS. Some of the parameters to evaluate the quality between strategies are as follows.

The first criteria is analisys the peaks of the maximum and minimum P_{Grid}, and these are defined by the positive and negative signs.

$$P_{Grid\ min} = min(P_{Grid}) \tag{7}$$

$$P_{Grid\ max} = max(P_{Grid}) \tag{8}$$

TABLE 5. Results of the quality criterion for P_{Grid}.

FL Strategy	$P_{Grid\ min}$	$P_{Grid\ max}$	MPD (W/h)	APD (W/h)	Energy G (J)
FLC NPT	-122157.27	3446.73	53171.11	4186.85	-2364692.58
FLC EROC	-859.91	7576.11	23077.04	872.146	4952734.99
FLC GF	-2070.68	1832.21	7777.99	491.48	-163824.84
FL EPC	-4470.59	2232.29	16050.12	1336.92	-2013381.4

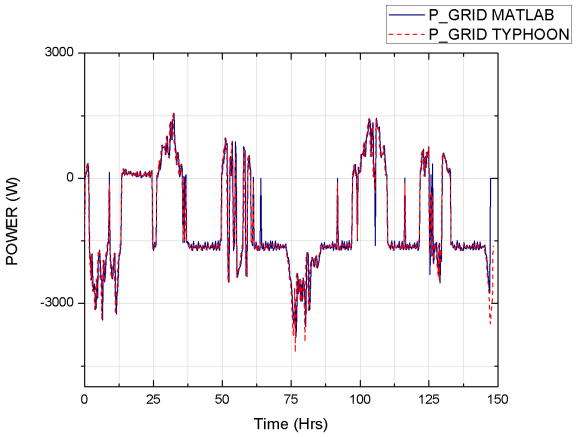

FIGURE 23. P_{Grid} FL EPC.

Another parameters is the maximum power bypass (MPD) which is defined as the range of maximum change in the main grid profile. In other words, it is the maximum absolute value of the slope during the sampling time represented by 9 [49]–[51]:

$$MPD = MAX(|\dot{P_G}|) \tag{9}$$

The third parameter used to define the quality of PMS is the average power derivative (APD) [22], which is defined as the absolute value of the average change in the period shown in the main grid profile; represented by the following [49]–[51]:

$$APD = \frac{1}{N}\sum_{n=1} N(|\dot{P_G}|) \tag{10}$$

In equation 9 and equation 10 the P_{Grid} is the reason for changing the power grid ($\dot{P_G}$), re-defined by the following formula:

$$\dot{P_G} = \frac{P_{Grid}(n) - P_{Grid}(n-1)}{T_S} \tag{11}$$

where n is the number of samples during the four months of data acquisition, T_S is the sampling time.

The numerical results previously obtained are shown in Table 5 and Table 6. The objetives defined to evaluate the quality in each of the strategies were APD and MPD for P_{Grid} and P_{Bat}. Another of the goals that are considered for the evaluation of PMS, are the peaks maximum and minimum for the P_{Grid}; finally, the point that is taken into consideration is the total of energy that each PMS delivers to the grid or to the BB.

TABLE 6. Results of the quality criterion for P_{Bat}.

FL Strategy	MPD BB (W/h)	APD BB (W/h)	Energy BB (J)
FLC NPT	83.057	5.79	2492255.94
FLC EROC	22778.55	1441.76	-5063990.3
FLC GF	3408.22	194.105	-58088.86
FL EPC	25823.08	1926.85	-2235295.2

Table 5 shows the criteria to evaluate in the P_{Grid} the first of these points to evaluate is the $P_{Grid\ min}$; the PMS that had lowest amplitude in this criterion was FLC EROC with a value of $859.91W$. The strategy with the amplitude in this same criterion was FLC NPT, with value of $122157.27W$. The second criterion evaluated was $P_{Grid\ max}$; the PMS registering the highest value was the FLC EROC strategy with a value of $7576.11W$; while FLC GF registers at the lowest amplitude in this criterion with $1832.21W$. These criteria of quality in the strategies indicate the range of operation.

The third point evaluated was the MPD, the FLC NPT strategy registers the highest value in this criterion with 53171.11 W/h, while the PMS with the lowest value is FLC GF with 7777.99 W/h. In fourth criterion APD, the PMS that obtained the maximum value is FLC NPT with a value of 491.48 W/h. Together these four criteria indicate the stability of PMS.

As an extra point for the PMS evaluated, it was taken as fifth criterion the sum of energy in P_{Grid}, remembering that the negative energy refers to an injection to the main grid, while a positive energy indicates use of the grid. The PMS that injected more energy is FLC NPT with $-2364692.58\ J$, while $-163824.84\ J$. Only the FLC EROC strategy record at the end a positive value of $4952734.99\ J$.

Table 6 shows some of the criteria applied to P_{Grid} to evaluate the quality of the energy in P_{Bat}, the first point is the MPD BB where the PMS registering the highest value is FL EPC with a value of 25823.08 W/h while the PMS with the value the lower the FLC NPT with a value of 83.957 W/h. The criterion APD BB the strategy with the highest value registered was FL EPC with 1926.85 W/h and the lowest value was 5.79 W/h which belongs to FLC NPT.

The third criterion used to evaluate the P_{Bat} is in totality of the energy, when it has a negative sign, it is interpreted that there was a charging process in the BB, on the other hand, when the energy has a positive sign, it is interpreted that there was a discharge process of the BB. The PMS reporting a load on the BB is FLC GF strategy with $-58088.86\ J$ while the FLC EPC reports the least amount of energy delivered to the BB with $-2235295.2\ J$.

VII. CONCLUSIONS

The proposed FL EPC has advantages compared with others PMS, such as small number of rules, fulfillment of the demanded power at every time, decreasing use of the storage unit, and keeping a balance between the different sources, storage unit and loads. This summary of characteristics opens its feasibility to be programmed in devices with limited resources.

Nevertheless, the few numbers of Fuzzy rules also generate practical limitations of the proposed PMS. For instance, it is second on the SOC criterion, and in the amount of energy injected into the main grid. Additionally, in the MPD and APD, the proposal has many changes, which in the long term, it can damage the end-user equipment. Future work will focus to overcome these limitations. One research direction is to change the triangular MF, in the Fuzzy proposal, with some other strategy. It was found that this waveform increases the system sensibility to sudden and less smooth changes. This will prevent the values in MPD and APD to be large, and it will increase the system's stability.

REFERENCES

[1] *Climate Change*. Accessed: Feb. 28, 2020. [Online]. Available: https://www.un.org/en/sections/issues-depth/climate-change/index.html
[2] *Introduction to Distributed Generation*. Accessed: Feb. 28, 2020. [Online]. Available: https://www.dg.history.vt.edu/ch1/introduction.html
[3] L. L. Grigsby, *Electric Power Generation, Transmission, and Distribution*, 3rd ed. Boca Raton, FL, USA: CRC Press, 2012.
[4] A. Ali, S. Padmanaban, B. Twala, and T. Marwala, "Electric power grids distribution generation system for optimal location and sizing—A case study investigation by various optimization algorithms," *Energies*, vol. 10, no. 7, p. 960, Jul. 2017.
[5] Y. Li, B. Feng, G. Li, J. Qi, D. Zhao, and Y. Mu, "Optimal distributed generation planning in active distribution networks considering integration of energy storage," *Appl. Energy*, vol. 210, pp. 1073–1081, Jan. 2018.
[6] D. Velusamy and G. K. Pugalendhi, "Fuzzy integrated Bayesian Dempster–Shafer theory to defend cross-layer heterogeneity attacks in communication network of smart grid," *Inf. Sci.*, vol. 479, pp. 542–566, Apr. 2019.
[7] A. Keshtkar and S. Arzanpour, "An adaptive fuzzy logic system for residential energy management in smart grid environments," *Appl. Energy*, vol. 186, pp. 68–81, Jan. 2017.
[8] M. L. Tuballa and M. L. Abundo, "A review of the development of smart grid technologies," *Renew. Sustain. Energy Rev.*, vol. 59, pp. 710–725, Jun. 2016.
[9] H. T. Haider, O. H. See, and W. Elmenreich, "A review of residential demand response of smart grid," *Renew. Sustain. Energy Rev.*, vol. 59, pp. 166–178, Jun. 2016.
[10] Z. Shuai, Y. Sun, Z. J. Shen, W. Tian, C. Tu, Y. Li, and X. Yin, "Microgrid stability: Classification and a review," *Renew. Sustain. Energy Rev.*, vol. 58, pp. 167–179, May 2016.
[11] C. Cecati, F. Ciancetta, and P. Siano, "A multilevel inverter for photovoltaic systems with fuzzy logic control," *IEEE Trans. Ind. Electron.*, vol. 57, no. 12, pp. 4115–4125, Dec. 2010.
[12] F. Chekired, C. Larbes, D. Rekioua, and F. Haddad, "Implementation of a MPPT fuzzy controller for photovoltaic systems on FPGA circuit," *Energy Procedia*, vol. 6, pp. 541–549, Jan. 2011.
[13] T.-F. Wu, C.-H. Chang, and Y.-H. Chen, "A fuzzy-logic-controlled single-stage converter for PV-powered lighting system applications," *IEEE Trans. Ind. Electron.*, vol. 47, no. 2, pp. 287–296, Apr. 2000.
[14] S. A. Khan and M. I. Hossain, "Design and implementation of microcontroller based fuzzy logic control for maximum power point tracking of a photovoltaic system," in *Proc. Int. Conf. Electr. Comput. Eng. (ICECE)*, Dhaka, Bangladesh, Dec. 2010, pp. 322–325.
[15] M. I. Hossain, S. A. Khan, M. Shafiullah, and M. J. Hossain, "Design and implementation of MPPT controlled grid connected photovoltaic system," in *Proc. IEEE Symp. Comput. Informat.*, Kuala Lumpur, Malaysia, Mar. 2011, pp. 284–289.
[16] Z. H. Jian, Z. Y. He, J. Jia, and Y. Xie, "A review of control strategies for DC micro-grid," in *Proc. 4th Int. Conf. Intell. Control Inf. Process. (ICICIP)*, Beijing, China, Jun. 2013, pp. 666–671.
[17] M. Borunda, O. A. Jaramillo, A. Reyes, and P. H. Ibargüengoytia, "Bayesian networks in renewable energy systems: A bibliographical survey," *Renew. Sustain. Energy Rev.*, vol. 62, pp. 32–45, Sep. 2016.
[18] F. Munteanu and C. Nemes, "Belief networks utilization for nodal power quality and availability assessment," *Univ. Politehnica Bucharest Sci. Bull., C, Elect. Eng.*, vol. 74, no. 1, pp. 215–222, 2012.
[19] A. Coleman and J. Zalewski, "Intelligent fault detection and diagnostics in solar plants," in *Proc. 6th IEEE Int. Conf. Intell. Data Acquisition Adv. Comput. Syst.*, Prague, Czeh Republic, Sep. 2011, pp. 948–953.
[20] A. Bashar, G. P. Parr, S. I. McClean, B. W. Scotney, M. Subramanian, S. K. Chaudhari, and T. A. Gonsalves, "Employing Bayesian belief networks for energy efficient network management," in *Proc. Nat. Conf. Commun. (NCC)*, Chennai, India, Jan. 2010, pp. 1–5.
[21] M. A. Teixeira and G. Zaverucha, "Fuzzy hidden Markov predictor in electric load forecasting," in *Proc. IEEE Int. Joint Conf. Neural Netw.*, Budapest, Hungry, Jun. 2004, pp. 315–320.
[22] D. A. Aviles, F. Guinjoan, J. Barricarte, L. Marroyo, P. Sanchis, and H. Valderrama, "Battery management fuzzy control for a grid- tied microgrid with renewable generation," in *Proc. 38th Annu. Conf. IEEE Ind. Electron. Soc. (IECON)*, Montreal, QC, Canada, Oct. 2012, pp. 5607–5612.
[23] S. K. Rathor and D. Saxena, "Energy management system for smart grid: An overview and key issues," *Int. J. Energy Res.*, vol. 44, no. 6, pp. 4067–4109, May 2020.
[24] H. Zhang, A. Davigny, F. Colas, Y. Poste, and B. Robyns, "Fuzzy logic based energy management strategy for commercial buildings integrating photovoltaic and storage systems," *Energy Buildings*, vol. 54, pp. 196–206, Nov. 2012.
[25] V.-H. Bui, A. Hussain, and H.-M. Kim, "A multiagent-based hierarchical energy management strategy for multi-microgrids considering adjustable power and demand response," *IEEE Trans. Smart Grid*, vol. 9, no. 2, pp. 1323–1333, Mar. 2018.
[26] L. Ju, Q. Zhang, Z. Tan, W. Wang, H. Xin, and Z. Zhang, "Multi-agent-system-based coupling control optimization model for micro-grid group intelligent scheduling considering autonomy-cooperative operation strategy," *Energy*, vol. 157, pp. 1035–1052, Aug. 2018.
[27] M. Molina-Solana, M. Ros, M. D. Ruiz, J. Gómez-Romero, and M. J. Martín-Bautista, "Data science for building energy management: A review," *Renew. Sustain. Energy Rev.*, vol. 70, pp. 598–609, Apr. 2017.
[28] T. Y. Ge, B. H. Zhang, J. L. Wu, B. J. Jin, S. Zhao, and K. M. Zhang, "Design of microgrid energy management system based on LabVIEW," *Adv. Mater. Res.*, vols. 960–961, pp. 1562–1566, Jun. 2014.
[29] H. Doukas, K. D. Patlitzianas, K. Iatropoulos, and J. Psarras, "Intelligent building energy management system using rule sets," *Building Environ.*, vol. 42, no. 10, pp. 3562–3569, Oct. 2007.
[30] F. Katiraei, R. Iravani, N. Hatziargyriou, and A. Dimeas, "Microgrids management," *IEEE Power Energy Mag.*, vol. 6, no. 3, pp. 54–65, May/Jun. 2008.
[31] F. Katiraei and M. R. Iravani, "Power management strategies for a microgrid with multiple distributed generation units," *IEEE Trans. Power Syst.*, vol. 21, no. 4, pp. 1821–1831, Nov. 2006.
[32] T. Morstyn, B. Hredzak, and V. G. Agelidis, "Control strategies for microgrids with distributed energy storage systems: An overview," *IEEE Trans. Smart Grid*, vol. 9, no. 4, pp. 3652–3666, Jul. 2018.
[33] F. J. Vivas, A. De las Heras, F. Segura, and J. M. Andújar, "A review of energy management strategies for renewable hybrid energy systems with hydrogen backup," *Renew. Sustain. Energy Rev.*, vol. 82, pp. 126–155, Feb. 2018.
[34] L. Olatomiwa, S. Mekhilef, M. S. Ismail, and M. Moghavvemi, "Energy management strategies in hybrid renewable energy systems: A review," *Renew. Sustain. Energy Rev.*, vol. 62, pp. 821–835, Sep. 2016.
[35] Y. Li and F. Nejabatkhah, "Overview of control, integration and energy management of microgrids," *J. Mod. Power Syst. Clean Energy*, vol. 2, no. 3, pp. 212–222, Aug. 2014.
[36] R. AhmadiAhangar, A. Rosin, A. N. Niaki, I. Palu, and T. Korõtko, "A review on real-time simulation and analysis methods of microgrids," *Int. Trans. Elect. Energy Syst.*, vol. 29, no. 11, pp. 1–16, Jun. 2019.

[37] W. A. Bisschoff and R. Gouws, "Energy management system for a residential grid-tied micro-grid," in *Proc. Int. Conf. Domestic Use Energy (DUE)*, Cape Town, South Africa, Mar./Apr. 2015, pp. 85–91.
[38] R. K. Chauhan, C. Phurailatpam, B. S. Rajpurohit, F. M. Gonzalez-Longatt, and S. N. Singh, "Demand-side management system for autonomous DC microgrid for building," *Technol. Econ. Smart Grids Sustain. Energy*, vol. 2, no. 1, pp. 1–11, Feb. 2017.
[39] J. Pascual, J. Barricarte, P. Sanchis, and L. Marroyo, "Energy management strategy for a renewable-based residential microgrid with generation and demand forecasting," *Appl. Energy*, vol. 158, pp. 12–25, Nov. 2015.
[40] D. Y. Yamashita, I. Vechiu, and J.-P. Gaubert, "A review of hierarchical control for building microgrids," *Renew. Sustain. Energy Rev.*, vol. 118, pp. 1–18, Feb. 2020.
[41] S. Leonori, M. Paschero, F. M. F. Mascioli, and A. Rizzi, "Optimization strategies for microgrid energy management systems by genetic algorithms," *Appl. Soft Comput.*, vol. 86, pp. 1–14, Jan. 2020.
[42] L. O. P. Vásquez, V. M. Ramírez, and K. Thanapalan, "A comparison of energy management system for a DC microgrid," *Appl. Sci.*, vol. 10, no. 3, pp. 1–14, Feb. 2020.
[43] J. Pascual, P. Sanchis, and L. Marroyo, "Implementation and control of a residential electrothermal microgrid based on renewable energies, a hybrid storage system and demand side management," *Energies*, vol. 7, no. 1, pp. 210–237, Jan. 2014.
[44] M. F. M. Sabri, K. A. Danapalasingam, and M. F. Rahmat, "A review on hybrid electric vehicles architecture and energy management strategies," *Renew. Sustain. Energy Rev.*, vol. 53, pp. 1433–1442, Jan. 2016.
[45] M. W. Khan, J. Wang, L. Xiong, and S. Huang, "Architecture of a microgrid and optimal energy management system," in *Multi Agent Systems Strategies and Applications*, R. Lopez-Ruiz, Ed. London, U.K.: IntechOpen, 2020, pp. 1–19.
[46] T. S. Ustun and S. M. S. Hussain, "Secure communication modeling for microgrid energy management system: Development and application," *Energies*, vol. 13, no. 1, p. 68, Dec. 2019.
[47] M. Kwon and S. Choi, "Control scheme for autonomous and smooth mode switching of bidirectional DC-DC converters in a DC microgrid," *IEEE Trans. Power Electron.*, vol. 33, no. 8, pp. 7094–7104, Aug. 2018.
[48] M. Coleman, W. G. Hurley, and C. K. Lee, "An improved battery characterization method using a two-pulse load test," *IEEE Trans. Energy Convers.*, vol. 23, no. 2, pp. 708–713, Jun. 2008.
[49] D. Arcos-Aviles, J. Pascual, L. Marroyo, P. Sanchis, F. Guinjoan, and M. P. Marietta, "Optimal fuzzy logic EMS design for residential grid-connected microgrid with hybrid renewable generation and storage," in *Proc. IEEE 24th Int. Symp. Ind. Electron. (ISIE)*, Buzios, Brazil, Jun. 2015, pp. 742–747.
[50] D. Arcos-Aviles, J. Pascual, L. Marroyo, P. Sanchis, and F. Guinjoan, "Fuzzy logic-based energy management system design for residential grid-connected microgrids," *IEEE Trans. Smart Grid*, vol. 9, no. 2, pp. 530–543, Mar. 2018.
[51] D. Arcos-Aviles, F. Guinjoan, J. Pascual, L. Marroyo, P. Sanchis, R. Gordillo, P. Ayala, and M. P. Marietta, "A review of fuzzy-based residential grid-connected microgrid energy management strategies for grid power profile smoothing," in *Energy Sustainability in Built and Urban Environments*. Singapore: Springer, 2019, pp. 165–199.
[52] D. Driankov, H. Hellendoorn, and M. Reinfrank, "The mathematics of fuzzy control," in *An Introduction to Fuzzy Control*, 2nd ed. Berlin, Germany: Springer, 2013, ch. 2, pp. 37–101.
[53] T. A. Runkler, "Extended defuzzification methods and their properties," in *Proc. IEEE 5th Int. Fuzzy Syst.*, New Orleans, LA, USA, vol. 1, Sep. 1996, pp. 694–700.
[54] M. Islam, F. Yang, C. Ekanayek, and M. Amin, "Grid power fluctuation reduction by fuzzy control based energy management system in residential microgrids," *Int. Trans. Elect. Energy Syst.*, vol. 29, no. 3, pp. 1–14, Mar. 2019.

JULIO C. PEÑA-AGUIRRE was born in Celaya, Guanajuato, Mexico. He received the B.Sc. degree in mechatronic engineering and the M.Sc. degree in electrical engineering from the Tecnológico Nacional de México en Celaya (TecNM en Celaya), in 2015 and 2017, respectively, where he is currently pursuing the Ph.D. degree. His research interests include control, instrumentation, and artificial intelligent.

ALEJANDRO-ISRAEL BARRANCO-GUTIÉRREZ (Member, IEEE) received the master's and Ph.D. degrees in advanced technology at CICATA IPN. He is currently working at the Cátedras - CONACYT, Department of Electronic Engineering, Technological Institute of Celaya, Celaya, Mexico. He is also a Telematics Engineer. His research interests include visual metrology, artificial intelligence, electronic circuits, and telematics.

JOSÉ A. PADILLA-MEDINA was born in Iguala, Guerrero, México. He received the bachelor's degree in electrical engineering from the Technological Institute of Celaya, México, in 1991, the M.Sc. degree in electrical engineering from Guanajuato University, in 1995, and the Ph.D. degree in optics from the Centro de Investigaciones en Óptica, in 2002. He is currently a Professor with the Department of Electronic Engineering, Instituto Tecnológico de Celaya, Tecnológico Nacional de México, Celaya, Mexico. He has published more than 40 scientific articles. His research interests include receiver operating characteristic (ROC) theory, visual perception, and applications of fuzzy logic and images processing.

ALEJANDRO ESPINOSA-CALDERON (Member, IEEE) received the Ph.D. degree in engineering from the Autonomous University of Queretaro, in 2012. He is currently designated as a National Researcher of Mexico, and a tenured Professor at the Centro Regional de Optimización y Desarrollo de Equipo, Tecnológico Nacional de México. His research interests include electronic instrumentation and digital signal processing applied to power electronics and biosystems.

FRANCISCO J. PÉREZ-PINAL (Senior Member, IEEE) received the M.Sc. degree in electrical engineering jointly from the University of Birmingham, Birmingham, U.K., and the University of Nottingham, Nottingham, U.K., in 2002, and the Ph.D. degree in electrical engineering from the University of San Luis Potosí, San Luis Potosí, Mexico, in 2008. He is currently a Professor at the Department of Electronic Engineering, Instituto Tecnológico de Celaya, Celaya, Mexico. His research interests include power electronics, energy conversion systems, and transportation electrification.